Lawrence Berkeley National Laboratory
Recent Work

Title
NUMERICAL SIMULATION OF EXPERIMENTAL DATA FROM PLANAR SIS MIXERS WITH INTEGRATED TUNING ELEMENTS

Permalink
https://escholarship.org/uc/item/52q372fc

Authors
Mears, C.A.
Hu, Q.
Richards, P.L.

Publication Date
1988-08-01

Lawrence Berkeley Laboratory
UNIVERSITY OF CALIFORNIA
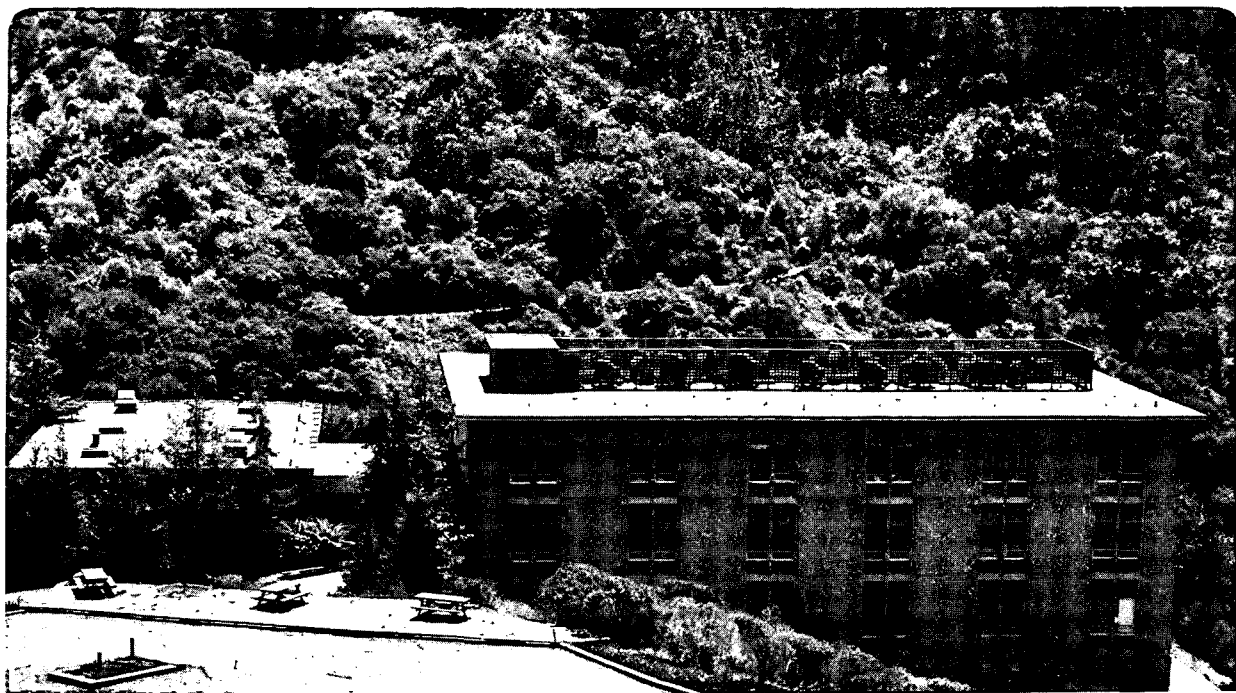
Materials & Chemical Sciences Division

Numerical Simulation of Experimental Data from Planar SIS Mixers with Integrated Tuning Elements

C.A. Mears, Q. Hu, and P.L. Richards

August 1988

DISCLAIMER

NUMERICAL SIMULATION OF EXPERIMENTAL DATA
FROM PLANAR SIS MIXERS WITH INTEGRATED TUNING ELEMENTS

C. A. Mears, Qing Hu, and P. L. Richards
Department of Physics, University of California

and

Materials and Chemical Sciences Division
Lawrence Berkeley Laboratory
Berkeley, California 94720

Abstract

We have used the full Tucker theory including the quantum susceptance to fit data from planar lithographed mm-wave mixers with bow tie antennas and integrated RF coupling elements.[1,2] Essentially perfect fits to pumped IV curves have been obtained. The deduced imbedding admittances agree well with those independently calculated from the geometry of the antenna and matching structures. We find that the quantum susceptance is essential to the fit and thus to predictions of the mixer performance. For junctions with moderately sharp gap structures, the quantum susceptance is especially important in the production of steps with low and/or negative dynamic conductance.

Introduction

SIS receivers have shown excellent performance at millimeter and submillimeter wavelengths. However, attempts to compare their behavior with the predictions of the Tucker theory of quantum mixing have met with limited success. In order to make a precise comparison between experiment and theory, the imbedding admittance at the signal, image, and intermediate frequencies must be known. These admittances have been measured accurately and used to predict performance in only a few cases[3] which cover a limited fraction of parameter space.

Several different methods have been used to determine the imbedding admittance. Many workers have constructed scale models of their mixer mount, but most have used these measurements only to test design concepts rather than to predict mixer performance. Alternatively, the mixer mount can be analyzed theoretically, but this is at best difficult. Probably the easiest way to determine the imbedding admittance is to fit measured pumped IV curves to those predicted by the Tucker theory, treating the imbedding admittance as a fitting parameter. Several workers have done this,[5-8] though in some cases the quality of the fit obtained was relatively poor. We have obtained fits that are essentially perfect, and thus we are confident that we have determined the imbedding admittance of our mixers quite accurately. Our mixer has no adjustable tuning structures. Instead we use fixed, planar lithographed tuning elements which have a frequency-dependent admittance that can be estimated from theoretical analysis of simple models, providing a basis for comparison with the parameters deduced from fitting of the pumped IV curve.

Photon-assisted tunneling

When electromagnetic radiation is incident on a tunnel junction, electrons can absorb or emit photons as they tunnel across the insulating barrier in a process known as photon assisted tunneling. The pumped dc current is given by[1,9]

$$I(V) = \sum_{n=-\infty}^{\infty} J_n^2(\alpha) \, I_{DC}(V_0 + n\frac{\hbar\omega}{e}), \quad (1)$$

where $\alpha = eV_{pump}/\hbar\omega$, V_{pump} is the amplitude of the LO voltage across the junction. $J_n(\alpha)$ is the nth order Bessel function of the first kind. $I_{DC}(V)$ is the DC current flowing through the unpumped junction at bias voltage V. If the junction is pumped by a voltage source, calculation of a pumped IV curve can be accomplished in a straightforward manner by evaluating this expression numerically. In the actual experimental situation, the junction is pumped by a source with a non-zero, complex output admittance. Tucker[1] has extended the theory of photon-assisted tunneling to include the case of arbitrary source admittance. In this theory, the input admittance of the junction varies with bias voltage, which causes the pump voltage to change with bias voltage. This changes the dynamic conductance of the steps on the pumped IV curve from that calculated for the voltage pumped case. Under the correct conditions this can give rise to steps of low or negative dynamic conductance, even for junctions with only moderately sharp current rises at the sum-gap voltage.

The dynamic conductance of these steps influences mixer performance in several ways. First, for DSB mixers, the IF output admittance is purely real and equal to the dynamic conductance of the pumped IV curve.[1] Secondly, the available gain has been shown to be roughly proportional to the dynamic resistance of the pumped IV curve.[10,11]

As pointed out by Smith et al, the dynamic conductance can be divided into two parts[12,13]

$$G_{dyn} = \sum_{n=-\infty}^{\infty} J_n^2(\alpha) \frac{\partial I_{DC}(V_0 + n\frac{\hbar\omega}{e})}{\partial V_0} + \quad (2)$$

$$\frac{d\alpha}{dV_0} \frac{\partial}{\partial \alpha} \sum_{n=-\infty}^{\infty} J_n^2(\alpha) I_{DC}(V_0 + n\frac{\hbar\omega}{e})$$

The first part is simply the dynamic conductance of the voltage pumped IV curve. This is almost always positive; it can only be negative near the gap voltage for a junction with a pronounced proximity effect induced super-gap structure.[14] We will ignore this case. The second part is due to the change in pump voltage with bias voltage. In order for steps of negative dynamic conductance to occur, this second term must be larger than the first term. We will show that for junctions with moderately sharp gap structures, this is primarily due to the change in the imaginary part of the input impedance of the junction at the LO frequency as the bias voltage is changed.

Role of quantum susceptance

In order to facilitate discussion, we will represent the junction and imbedding structure with an equivalent circuit identical to the circuit in reference 1. The junction is assumed to be driven by a current source at the local oscillator frequency. The imbedding admittance at the LO frequency ($Y_{IMB} = G_{IMB} + jB_{IMB}$) includes both the imbedding structures and the geometrical capacitance of the junction. The junction admittance at the LO frequency ($Y_J = G_J + jB_J$) includes only the "quantum" admittance, i.e. that calculated using Tucker's quantum theory of photon assisted tunneling.

In order to gain some physical insight into the nature of the terms G_J and B_J, it is instructive to first consider the case of very low pump power. In this case, we only keep terms in the lowest non-vanishing power of the reduced pump voltage α. The in-phase and out-of-phase components of the local oscillator current[1]

$$I_{LO} = (I'_{LO} + jI''_{LO})e^{-j\omega t}$$

$$I'_{LO} = \sum_{n=-\infty}^{\infty} J_n(\alpha)[J_{n-1}(\alpha) + J_{n+1}(\alpha)] I_{DC}(V_0 + n\frac{\hbar\omega}{e}) \quad (3)$$

$$I''_{LO} = \sum_{n=-\infty}^{\infty} J_n(\alpha)[J_{n-1}(\alpha) - J_{n+1}(\alpha)] I_{KK}(V_0 + n\frac{\hbar\omega}{e})$$

reduce to

$$I'_{LO} = \frac{e}{\hbar\omega}\left[I_{DC}(V_0 + \frac{\hbar\omega}{e}) - I_{DC}(V_0 - \frac{\hbar\omega}{e}) \right]$$

$$(4)$$

$$I''_{LO} = \frac{e}{2\hbar\omega}\left[I_{KK}(V_0 + \frac{\hbar\omega}{e}) - 2I_{KK}(V_0) + I_{KK}(V_0 - \frac{\hbar\omega}{e}) \right]$$

where $I_{KK}(V)$ is the value of the Kramers-Kronig transform of the DC IV curve at voltage V. It can be seen that these currents depend on I_{DC} and I_{KK} only at points spaced by nV_{LO} above and below the bias point. These points are refered to as photon points. Dividing the LO current by the pump voltage, we obtain the low power conductance and susceptance of the junction.

The RF conductance G_J is equal to the first finite difference of I_{DC} calculated at the first photon points above and below the bias point. At a bias point more than V_{LO} below the gap the conductance is small. Within V_{LO} of the gap on each side, the RF conductance is large compared to the junction normal conductance G_N. In this range, it is approximately equal to the magnitude of the sum-gap current rise divided by twice V_{LO}. More than V_{LO} above the gap, the RF conductance is approximately equal to G_N. The exact behavior near the boundaries of the these regions depends on the exact shape of the current rise, but in general is smooth and monotonic. The important point is that while the RF conductance changes dramatically between steps, it is relatively constant on the first sub-gap and super-gap steps.

The susceptance is equal to the second finite difference of the I_{KK} calculated at the bias point and the first photon points above and below the bias point. The susceptance is positive (capacitive) for bias voltages more than V_{LO} away from the sum-gap. Near the gap, however, the susceptance varies violently with bias voltage because the photon points straddle the cusp in I_{KK} that occurs at the sum-gap voltage. As the bias voltage is increased across the first step below the sum-gap voltage, the susceptance changes from being positive (capacitive) and small to being negative (inductive) and large. No simple estimate can be made for the maximum and minimum values of the susceptance because these depend explicitly on the height of the cusp in I_{KK}, which decreases rapidly with increasing width of the current rise at the sum-gap voltage. For the moderately sharp junction used in this work, the maximum value was 1.0 times G_N, and the minimum value was -2.0 times G_N. It is important to notice that while the conductance stays essentially constant across the first photon step, the susceptance changes considerably.

If we consider the conductance to be constant across a step, it is easy to see how the susceptance is responsible for the variation
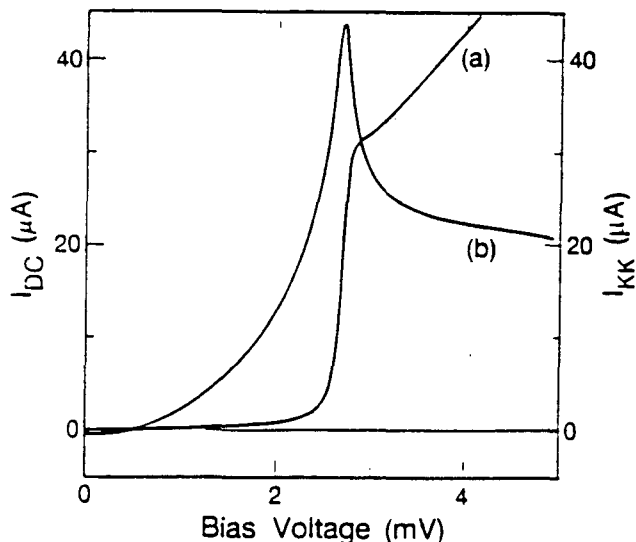

Figure 1. a) DC IV curve of the junction used in this work.
b) Kramers-Kronig transform of the DC IV curve.

of pump voltage. If $B_{IMB} = -B_J$ no net current flows through the susceptive part of the equivalent circuit. This leads to a high pump voltage. If B_{IMB} and B_J have the same sign, or are very different in magnitude, current is shunted through the susceptive elements, and the corresponding pump voltage is low. If the B_{IMB} is slightly negative, i.e. slightly inductive, then B_{IMB} will be equal to B_J on the lower bias voltage part of the first step, leading to a high pump voltage there, and B_{IMB} will be of the same sign as B_J on the higher part of the first step, leading to a low pump voltage there. The opposite is true for a slightly capacitive imbedding admittance.

With large pump power, the situation becomes more complicated. The LO currents are no longer linearly dependent on the pump voltage. In order to calculate the LO currents, the pump voltage must be calculated numerically at each bias point, and then substituted into the expressions (3) for the LO currents. The results of this calculation for a junction of moderate quality are shown in figure 2. Two different imbedding admittances are used to illustrate general trends. Notice that the shapes of the junction conductance and susceptance curves for both cases are similar to those described in the previous section. The junction conductance is relatively constant on a step, but changes rapidly between steps. The susceptance, however changes rapidly on the first sub-gap and super-gap steps. It is this change that is responsible for the significantly different dynamic conductance on the steps of the two pumped IV curves. Now we will focus our attention to the first sub-gap step, and explain the differences that result from the capacitive and inductive imbedding admittances.

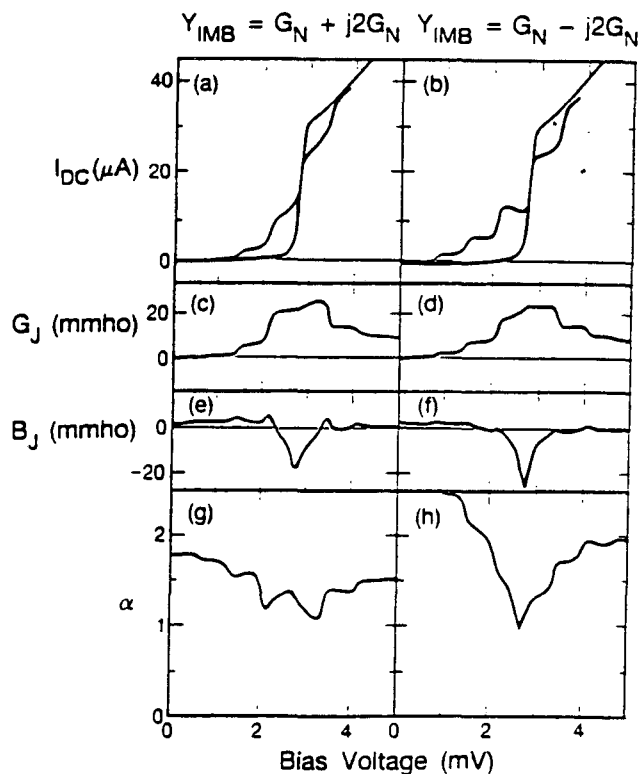$$Y_{IMB} = G_N + j2G_N \qquad Y_{IMB} = G_N - j2G_N$$

Figure 2. a), b) DC and Pumped IV curves. c), d) RF Junction conductance. e), f) RF Junction susceptance. g), h) reduced pump voltage. All quantities are shown two different imbedding admittances. The LO frequency is 160 GHz in both cases.

In the capacitive case, there is considerable mismatch at the lower end of the first sub-gap step, while B_J resonates B_{IMB} at the upper end of the same step. Notice that the reduced pump voltage α increases with bias voltage across this step. Thus $d\alpha/dv$ is positive, and both terms in equation (2) are positive, leading to a large dynamic conductance.

In the inductive case, there is some mismatch at the lower end of the step, but this mismatch increases at the upper end of the step, leading to a reduction of α across the step. In this case, $d\alpha/dv$

is negative and large enough to cause the second term in equation (2) dominate the first, and the dynamic conductance on the step is negative.

Calculations were also carried out using the same DC IV curve in which the out of phase currents flowing in the junction were ignored. Negative dynamic conductance was only observed when the real part of the imbedding admittance was very low. $G_{IMB} < 0.1$ G_N, as opposed to $G_J = G_N$ in figure 2. The negative conductance only appeared at the extreme low bias voltage end of the first sub-gap step, in a region that is actually between the first and second sub-gap steps. We have never experimentally observed negative dynamic conductance in this region.

We therefore conclude that the susceptance due to out-of-phase currents flowing in the junction is essential in the production of steps of low or negative dynamic conductance in junctions with moderately sharp sum-gap current rises. In high quality junctions, the quantum susceptance probably plays an even more dominant role because of the larger cusp in the Kramers-Kronig transform of the DC IV curve, which causes an even larger swing in the quantum susceptance across a step.

Description of Experimental Tuning Structures

We have designed and evaluated planar lithographed W-band SIS mixers with integrated RF coupling structures.[2] Nb/NbO$_X$/Pb-In-Au junctions were fabricated with $\omega R_n C \gg 1$. The junctions are located at the apex of a 90 degree bow tie antenna which is deposited on a fused quartz substrate, which in turn forms part of 12.7 mm diameter hemispherical fused quartz lens. In order to resonate the junction capacitance at the signal frequency, an open circuited microstrip stub was connected in parallel with the junction. The susceptance of the microstrip stub can be written as $B = Y_0$ tan($\omega l/v$), where Y_0 is the characteristic admittance of the line, v is the phase velocity of the line, and l is the line length. The characteristic admittance is chosen such that $\omega C/Y_0 = 1$ to maximize bandwidth of the fundamental resonance. The line is constructed as in Ref. 2 with a phase velocity of 0.30c, characteristic admittance of 0.1 mho, and a length of 0.38mm to give a resonant frequency of 90 GHz for a 0.16 pF junction. Mixers with microstrip stubs designed to resonate at 180, 270, and 360 GHz have also been constructed.[15]

The imbedding admittance seen by the bare junction is the parallel combination of the output admittance of the antenna, the admittance of the stub, and the admittance due to the geometrical capacitance of the junction. A plot of the expected imaginary part of the imbedding admittance is shown in figure 4. The real part is expected to be a constant equal to the output conductance of the bow tie antenna, which is frequency independent.

Fitting of Experimental Admittances

In order to deduce the actual imbedding admittances present in the experiment, we have fit the experimental pumped IV curves to theoretically calculated pumped IV curves. By varying the imbedding admittance and the available pump power we were able to obtain almost perfect fits. In order to automate the fitting procedure, contour plots of the absolute difference between the experimental and calculated pumped IV curves were computed as a function of imbedding admittance. The absolute difference was computed at only six representative points to minimize computation time. The minimum value of the sum of absolute differences was usually between 0.5 and 0.2 microamps. All contour plots computed exhibited a single minimum. Near the resonant frequency, these minima were well defined, and the uncertainty in imbedding admittance is small. At frequencies above and below the resonant frequency, the minima tended to be very elliptical, leading to a larger uncertainty in fitted imbedding admittance. Pumped IV curves computed with imbedding admittances that fell within the contour 0.2 microamps from the minimum value were visually indistinguishable from each other.

Fits obtained were of quite high quality. A typical example is shown in figure 3. By varying the geometrical capacitance of the junction and the phase velocity of the transmission line, the expected imbedding susceptance could be fit to the imbedding susceptance deduced from the pumped IV curves, as shown in figure 4. The fitted values for the capacitance and phase velocity were 0.50 pF and 0.34 c, in good agreement with estimated values of 0.38 pF and 0.32 c. The estimated value of the capacitance was calculated from the junction area, the thickness and dielectric
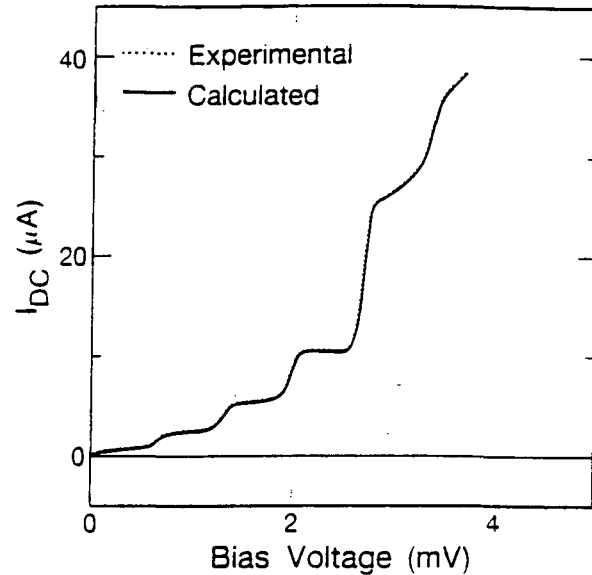

Figure 3. Experimental and Calculated pumped IV curve. The experimental data points are offset upward by 0.02 μA. The LO frequency is 161 GHz.
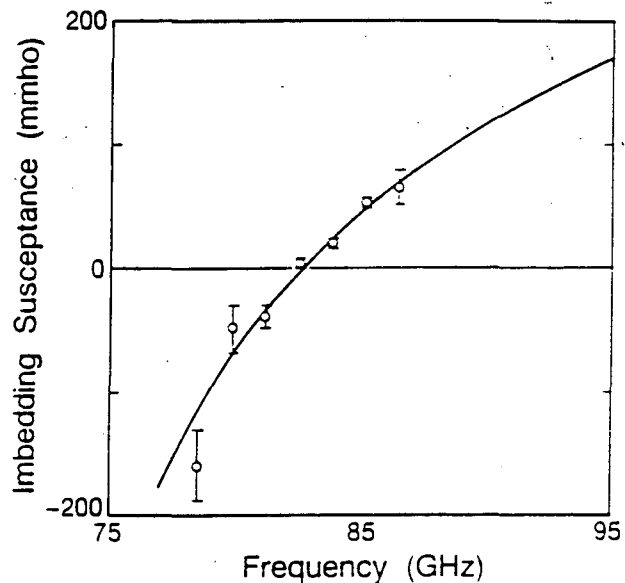

Figure 4. Deduced imbedding susceptance as a function of frequency for single junction with bow tie antenna and microstrip tuning stub. The solid line is calculated using a geometrical junction capacitance of 0.50 pF, and a microstrip phase velocity of 0.34 c.

constant of the tunneling barrier. The phase velocity in the microstrip stub was estimated using the thickess of the dielectric, its dielectric constant, and the penetration depth of the superconductors.

The imbedding conductance was expected to be a constant equal to the output conductance of the bow tie antenna. Above the resonant frequency the deduced imbedding conductance agrees well with this expectation. Below the resonant frequency the conductance rises rapidly with decreasing frequency. A simple model with a frequency independent loss per unit length in the stub qualitatively fits this behavior. The possibility of such a loss is currently under investigation.

References

[1] J. R. Tucker, "Quantum Limited Detection in Tunnel Junction Mixers," IEEE J. Quantum Electronics, vol. QE-15, pp. 1234-1258, 1979.

[2] Li Xizhi, P. L. Richards, and F. L. Lloyd, "SIS Quasiparticle Mixers with Bowtie Antennas," Int. J. Infrared and Millimeter Waves, Vol. 9, pp 101-133, 1988.

[3] M. J. Feldman, S. K. Pan, A. R. Kerr, and A. Davidson, "SIS Mixer Analysis Using a Scale Model," IEEE Trans. Magn., vol. MAG - 17, pp. 494-497, 1983.

[4] R. L. Eisenhart, and P. J. Khan, "Theoretical and Experimental Analysis of a Waveguide Mounting Structure," IEEE Trans. Microwave Theory Tech.,vol. MTT-19, pp. 706-719, 1971.

[5] T. M. Shen, P. L. Richards, R. E. Harris, and F. L. Lloyd, "Conversion Gain in Millimeter Wave Quasiparticle Heterodyne Mixers," Appl. Phys. Let.,Vol. 36, pp. 777-779, 1980.

[6] T. G. Phillips and G. J. Dolan, "SIS Mixers," Physica, vol. 109 and 110B, pp. 2010-2019, 1982.

[7] A. Skalare, J. Johansson, E. Kollberg, and R. Murowinski,"Integrated Slot Line Antenna with SIS Mixer for Focal Plane Array Applications," Preprint, 1987.

[8] W. R. McGrath, P. L. Richards, D. W. Face, D. E. Prober, and F. L. Lloyd, "Accurate Experimental and Theoretical Comparison Between Superconductor-Insulator-Superconductor Mixers Showing Weak and Strong Quantum Effects," J. Appl. Phys, Vol. 63, pp. 2479-2491, 1988.

[9] P. K. Tien and J. P. Gordon, "Multiphoton Process Observed in the Interaction of Microwave Fields with the Tunneling Between Superconducting Films," Phys. Rev, Vol. 129, pp. 647-651, 1962.

[10] J. R. Tucker, "Predicted Conversion Gain in Superconductor-Insulator-Superconductor Quasiparticle Mixers," Appl. Phys. Lett., vol 36, pp. 477-479, 1980.

[11] T.-M. Shen and P. L. Richards, "Computer Simulations of the Performance of Quasiparticle Heterodyne Mixers," IEEE Trans.Mag., vol. MAG-17,pp 677-683, 1981.

[12] A. D. Smith, W. R. McGrath, P. L. Richards, H. van Kempen, D. E. Prober, and P. Santhanam, "Negative Resistance and Conversion Gain in SIS Mixers," Physica B+C, Vol. 108, pp. 1367-1368, 1981.

[13] A. D. Smith and P. L. Richards, "Analytic Solutions to Superconductor-Insulator-Superconductor Quantum Mixer Theory," J. Appl. Phys., vol 53, pp. 3806-3812, 1982.

[14] E. L. Wolf, Principles of Electron Tunneling Spectroscopy, Oxford Press, 1985.

[15] Qing Hu, C. A. Mears, P. L. Richards, and F. L. Lloyd, "MM Wave Quasioptical SIS Mixers," to be published in these proceedings, 1988.